NI

NASA Technical Memorandum 82849

Environmentally Induced Discharges on Satellites

N. John Stevens
Lewis Research Center
Cleveland, Ohio

Prepared for the
Second EMC Seminar
sponsored by ESTEC
Noordwijk, The Netherlands, May 11-13, 1982

ENVIRONMENTALLY INDUCED DISCHARGES ON SATELLITES

by N. John Stevens

National Aeronautics and Space Administration
Lewis Research Center
Cleveland, Ohio, USA

E-1219

ABSTRACT

The problem of assessing hazards to geosynchronous satellite systems from geomagnetic substorm encounters has plagued investigators for several years. Electronic switching anomalies have been occurring on satellites and appear to be related to environmental charging. Yet, if the assumed large differential voltage type of discharge were involved, then there should have been more catastrophic failures. The available space flight data, coupled with analytical modeling studies, have shown that only relatively low differential charging is possible from environmental encounters. Using an analytical study of a discharge event on SCATHA, a discharge process is postulated where a small amount of charge is lost to space. These characteristics could then be used as inputs to a coupling model to determine the hazard to a spacecraft. The procedure is applied to a three-axis stabilized satellite design.

INTRODUCTION

Since 1975, a combined Air Force/National Aeronautics and Space Administration investigation has been underway to understand and control a phenomenon known as "spacecraft charging" (Ref. 1). This charging occurs when geosynchronous satellites encounter geomagnetic substorm environments resulting in the deposition of charge on satellite exterior surfaces (Ref. 2). This phenomenon was observed as a result of experiments on ATS-5 in 1969. Here, data from the Auroral Particles Experiment showed that substorm environments could charge satellite structures to large negative values (Ref. 3). These initial results have been confirmed and expanded upon by data from instruments on ATS-6 and SCATHA (Refs. 4 and 5). The differential charging of the dielectric surfaces of geosynchronous satellites appears to become large enough to cause breakdowns and the resulting transients couple into the electrical system producing switching anomalies. The existence of such exterior breakdowns and resulting transients on satellite harnesses has been shown by monitors on satellites (Refs. 6 and 7). While satellites have been in geosynchronous orbit since the mid-sixties, the anomalous occurrences seem to arise when manufacturers converted from latching relay logic to computer level logic (Ref. 8).

The initial phases of the AF/NASA investigation centered on the concept that large differential voltages between sunlit and shaded surfaces would exist under typical substorm conditions (Ref. 9). At projected differential voltages (>10 kV), laboratory tests indicated that spectacular, visible breakdowns or discharges were possible (Ref. 10). Transient current surges of 0.5 ampere per square centimeter of dielectric area were measured. Extrapolating current surges to spacecraft sizes resulted in huge effects which should have destroyed satellites (>1000 A pulses). In the 13 years since this phenomenon has been tracked, only one possible failure can be ascribed to spacecraft charging effects (Ref. 11). Most of the anomalies are a result of spurious command switching and noisy telemetry.

Analytical modeling studies (Ref. 12) and space flight data from SCATHA (Ref. 13) and ATS-6 (Ref. 14) have shown that large differential charging just does not occur on satellites in geosynchronous orbits. Therefore, the conditions necessary to produce the large area breakdowns observed in the laboratory do not exist in space conditions. Yet, transients are observed on satellites. Hence, there must be some process associated with geomagnetic substorm environments that can produce breakdowns at the observed lower differential voltages.

This paper explores the possibility of low differential voltage breakdowns on geosynchronous satellites. First, modeling results on different types of satellites are shown to demonstrate the range of differential voltages that could be expected. Then, a transient event that occurred on SCATHA during eclipse charging is used to develop a concept for a possible discharge model. This model is then proposed and the resultant transient characteristics computations postulated. Finally, this discharge model is applied to a three-axis stabilized satellite.

DIFFERENTIAL CHARGING OF SATELLITES

As a means of demonstrating that the possible differential voltage on satellites cannot reach the high values required for large discharges, two different satellite configurations are analyzed with the NASA Charging Analyzer Program (NASCAP). NASCAP is a three-dimensional code and is fully capable of describing transient and steady-state charging behavior (Refs. 15 to 18).

Both a three-axis stabilized and spin-stabilized satellite have been chosen for this demonstration

since it has been shown that configurations do influence charging behavior (Ref. 19). The NASCAP models of these satellites are shown in figure 1. The three-axis-stabilized satellite chosen is the NASA Tracking and Data Relay Satellite System (TDRSS) that will replace existing ground stations. It is a large satellite, 18.9 by 11.7 meters in overall dimensions. It consists principally of two large solar arrays, two main antennas, two smaller antennas and the spacecraft body. The materials chosen for this study simulate the actual coatings. The two main antennas were modeled as an octagonal rim with a central rectangular feed in order to evaluate the charging of the optical solar reflectors (OSR's) covering the electronic enclosure behind the antenna feed. Since the antenna mesh was transparent, there was a possibility of part being sunlit while the rest was shaded. The backing of the solar arrays was assumed to be plain Kapton. The spinning satellite chosen is the P78-2 Spacecraft Charging at the High Altitudes (SCATHA) satellite. It has cylindrical sides covered primarily with solar arrays and uses appropriate dielectrics on the "belly band," top and bottom surfaces.

A design evaluation environment (Ref. 20) was used in this study. The Sun incidence for the TDRSS evalution was offset such that the viewer would be looking at the model from the Sun. For the SCATHA evaluation, the Sun was assumed to be normal to the solar array and the satellite to be spinning at 1 rpm.

The results predicted for satellite grounds and shaded Kapton insulation areas are shown in figure 2. The three-axis-stabilized spacecraft ground is charged more negatively both in sunlight and eclipse than the spinning satellite ground. This is due to the large areas of shaded insulation behind the solar arrays, which charge to high negative values and thus create fields surrounding the satellite, reducing photoemission. The spinning satellite tends to average this shading effect and thus maintains a lower ground potential.

The maximum differential voltage between the satellite ground and dark insulators ranges between 1.5 and 3.0 kV for both satellites. At these differential voltages, laboratory tests conducted with substrates grounded would indicate no possibility of discharges: the insulators would simply be mildly charged (Ref. 21). Hence, it is necessary to develop a method of predicting when discharges could occur under realistic space conditions and determining what their characteristics would be. The SCATHA data can be used to assist in this study.

ENVIRONMENTALLY-INDUCED DISCHARGES ON SCATHA

Background

The P78-2 or SCATHA satellite was launched in 1979 into a slightly elliptic orbit to collect data on spacecraft charging interactions (Ref. 11). It is a cylindrical spacecraft with several booms. Instrumentation on-board was designed to measure the space environmental parameters and satellite responses to this environment. It spins at 1 rpm. The satellite has been successful in meeting its objectives (Refs. 22 and 23).

The summaries of the Satellite Surface Potential Monitor (SSPM) data have shown that there has been relatively low differential charging on the dielectric samples (Ref. 24). Differential charging seems to be limited to values of about 2 kV even though the satellite has been charged to -10 kV in eclipse. Even with this mild differential voltage, discharges have been observed which are attributed to environmental charging (Ref. 25). The amplitude of these discharge transients tend to be less than a volt, indicating a relatively low charge loss. The location of these discharges have not been identified.

For the eclipse charging event on March 28, 1979, the NASCAP computer code has been used to generate surface voltage predictions for comparison to flight data. The computer model, shown in figure 1, was used along with the environmental data provided from the particle detectors to predict the satellite ground potentials (Ref. 26). The comparison is very favorable (see fig. 3). The rms temperature data, available at only discreet intervals shows an initial environmental pulse to 11 KeV and then stabilization between 5 and 6 KeV. The computer predictions for the ground potentials (short dashed lines) follows the measured values very well. A detailed comparison of the predictions to the measured values of voltage and current of the large Kapton sample on the SSPM is also excellent (Ref. 27). Hence, NASCAP can predict reasonable values for absolute and differential charging on SCATHA at least in this substorm.

A review of the surface charging voltage predictions from this NASCAP computer run, did not reveal any large differential charging. One would have expected that the satellite was charged as a unit in the initial phase of the substorm and that whatever differential voltages developed would have occurred in the milder phases of the substorm. Yet, a discharge did occur within 100 seconds after encountering the substorm (Ref. 25). Furthermore, there were no more discharges, even though the substorm intensified, until 90 seconds after the satellite entered sunlight.

Proposed Discharge Model

In this section a model is proposed to explain the fact that the March 28, 1979 discharge event could have occurred at about 100 seconds after the initial substorm encounter and why it was not repeated in the more intense portions of the storm. This model assumes that the discharge occurred at the boom tips where a metal sphere was attached to a dielectric-coated boom (see fig. 4). The comparison of predictions to data, mentioned previously for this event did indicate that the boom dielectrics were at the structure voltage which was more positive than the metal sphere. This condition can produce discharges (Refs. 28 and 29). It is also assumed that the metal shell is only capacitively coupled to the boom and not hard-wired to structure ground. The capacitance value was arbitrarily chosen to be 2×10^{-10} F.

Hence, the model considered is essentially three capacitances: from the shell to space (C_1) from the shell to spacecraft body (C_2) and from the body to space (C_3). When a discharge is triggered, a small amount of charge is assumed to be lost to space from the shell and the body will respond according to the capacitances linking it to the shell and space (see fig. 5). For this simple model, then, for any assumed charge loss from the shell to space, the change in voltage of the shell could be computed.

$$\Delta V_{shell} = \frac{\Delta Q_{loss}}{C_1}$$

The response of the body then would be the ratio of the capacitances times the change in shell voltages.

$$\Delta V_{body} = \frac{C_1}{C_{eff}} \Delta V_{shell}$$

where C_{eff} is the effective capacitance of C_2 and C_3 in series. Since C_{eff} is larger than C_1, the change in body voltage is less than that of the shell and hence, the discharge should not be repeated unless the substorm persisted at relatively high intensity for longer than the original 100 seconds.

It is further assumed that this charge-loss process is triggered when the metal surface becomes 500 to 1000 volts more negative than the surrounding dielectrics. The process is assumed to be quenched when the metal surface goes to zero volts and charging is again initiated.

While it is possible to compute the change in voltages for given charge loss, it is not possible to do a valid simulation of a charging-discharging cycle without a three-dimensional code. For this simulation of the above model, the NASCAP code is used to predict the surface charging and recharging at the time of the actual discharge occurrence. Using the available environment data and a SCATHA model with a floating boom tip experiment ($C_1 = 2X10^{-10}$ F), the computer simulation was run up to the approximate time of discharge (98.4 sec). The differential voltage between the boom tip (of the SCATHA model) and the boom dielectric was about 1000 volts with the tip more negative. At this time 0.37 μcoulombs of charge was instantaneously lost to space from the tip by specifying this transfer in the code. The amount chosen was that necessary to change the tip voltage to zero and represented 65 percent of the total charge stored on the tip. The code computed the change in all surface potentials due to this loss and then allowed the surfaces to be recharged by the environment. For this example, the code predicted that the structure would return to its previous value in less than 1 second - fast enough to imply that most of the satellite instrumentation might have missed the change.

The discharge transients in the tip and structure for this simulated event are shown in figure 6. Just prior to the discharge, the boom dielectric surfaces (dielectric surface voltages are the same as the structure) are considerably less negative than the tip. At the approximate time of discharge, the environment appears to have become more intense causing an increase in the charging rate and probably triggering the discharge. When these conditions are simulated by NASCAP, the expected inversion between the tip and structure potential occurs. The predicted voltage distributions around the satellite emphasize the effect of this transition (see fig. 7). In figure 7(a), the potential distributions around the satellite just prior to discharge are shown. At the time of discharge (fig. 7(b)), the voltage levels change, but only at the floating tip are there significant deviations in the pattern. After recovery (fig. 7(c)), the voltage distribution around the tip is still the only area where significant changes in the pattern have occurred. It appears, then, that this simulation produced the desired, highly localized transient.

The question of why discharges were not repetitive can be addressed by a continuation of the charging simulation through the peak intensity of the substorm (see fig. 8). In figure 8(a), the charging history for the predicted structure ground and boom tip is shown without the discharge simulation. As shown, the presumed conditions for triggering a discharge exist at 98 seconds, 110 seconds, and 120 seconds into the substorm encounter. However, when the discharge was simulated at 98 seconds (fig. 8(b)), the resultant inversion of tip and structure persisted throughout the peak and the conditions for discharge were not repeated. Had the substorm intensity continued for a longer period of time, then the differentials would have been re-established and another discharge could have occurred.

DISCUSSION

The model proposed to explain the discharge occurrence on SCATHA can be generalized to other satellites. In essence, it is proposed that a discharge occurs when charge is lost to space by a breakdown of the capacitance to space. The response of other parts of the satellite depends upon the capacitive coupling to the discharge site and to space.

The discharge process has been assumed to be initiated when a metal surface is at least 500 volts more negative than the surrounding dielectric surfaces in agreement with laboratory data (Refs. 28 and 29). Yet, there are other conditions that could give rise to a discharge which are related to a negative voltage gradient at a dielectric-conductor interface (Refs. 30 and 31). These did not occur in the SCATHA example but must be considered in any, more generalized model.

Finally, it should be pointed out that a discharge could occur on the body of a satellite. In this case, the structure potential would go to zero volts directly, there would be no inversion process, and repetitive discharges are very likely. In the next section of this report, all of these concepts are melded into a generalized, proposed surface breakdown model.

ENVIRONMENTALLY-INDUCED SURFACE BREAKDOWN MODEL

For a complete evaluation of any geosynchronous satellite, the effects of surface breakdown (discharges) transients caused by environmentally-induced charging should be ascertained. This evaluation requires knowledge of breakdown trigger conditions and a discharge process to determine transient characteristics. This would be the first step in an analysis to determine the systems response to discharges. The discharge characteristics resulting from the surface breakdown would be used as inputs for codes to compute the internal structural response (e.g., SEMCAP). The calculation of internal response tends to be configuration dependent and cannot be treated in a general manner.

Based on the current state of knowledge and the results of the study in the previous section, provisional criteria for breakdown initiation can be proposed. These criteria are:

(a) Dielectric surface voltages are greater than +500 volts relative to an adjacent exposed conductor (Refs. 28 and 29).

(b) A dielectric/exposed conductor interface has an electric field greater than 1×10^6 volts/cm (Refs. 30 and 31).

Gaps, seams, edges, and imperfections enhance the existence of these conditions and thereby increase the probability of breakdowns. It is assumed that these discharges result in a relatively small charge loss to space.

The discharge process proposed is that charge is transferred from the satellite to space; in essence satellite to space plasma ground is temporarily shorted. (see fig. 9(a)). It is assumed that a breakdown continues until the satellite ground potential approaches space plasma potential as indicated by ground simulation experiments (Ref. 32). Accompanying this voltage transient is a local collapse of differential voltages at the discharge site. Charge is not drained off of large areas of dielectrics as previously assumed (Ref. 21) but some small fraction of the total stored charge is assumed to be lost to space in this differential voltage collapse. The remaining charged dielectrics force the ground potential to return rapidly towards its precharged value.

Discharge transients can be computed as follows:

(1) The square wave approximation for the current transient is derived from the total charge lost over the same period. This charge lost is made up of two parts:

(a) The charge lost to space through the satellite to space capacitor is computed from (see fig. 9(b)):

$$\Delta Q = C_s V_o \qquad \text{(Coulombs)}$$

where C_s is the satellite to space capacitor (typically 10^{-10} farads) and V_o is satellite ground voltage at time of discharge.

(b) In order to compute the charge lost in the dielectric differential voltage collapse, one has to rely on laboratory results obtained from grounded substrate tests. These tests produced discharges which removed charge from large areas of the dielectric surface, but it is believed that the initiation of the transient is the same for floating substrate discharges. For the present, then, charge redistribution and time duration relationships from these tests will be used. Additional testing should be undertaken to obtain data on discharge characteristics with floating substrates.

It is assumed that only 1 percent of the total charge stored on the dielectric surface is involved in this portion of the discharge process. This is an arbitrary assumption made to stress the fact that charge loss is limited to a small dielectric area. Of this 1 percent, only 1/3 is lost to space; the remaining 2/3 either stays on the dielectric or neutralizes the polarization charge: (Ref. 33)

$$\Delta Q_2 = K C_D \Delta V_D \qquad \text{(Coulombs)}$$

where:

K is the friction of total charge lost to space (0.003)
C_D is the dielectric capacitance (farads)
ΔV_D is the absolute value of differential voltage across dielectric (volts)

(c) Hence, the total charge lost is:

$$\Delta Q_L = \Delta Q_1 + \Delta Q_2 \qquad \text{(Coulombs)}$$

and the current pulse is:

$$I = \Delta Q_L / \Delta t \qquad \text{(Amps)}$$

The time duration of this pulse (Δt) is not known. The experimental data for grounded substrate tests indicate that the maximum duration is a function of dielectric area from which charge has been removed (Ref. 33). Using this relationship, a time duration can be approximated as:

$$\Delta t \sim 0.02 (K_2 A_D)^{0.5} \qquad (\mu\text{sec})$$

where

K_2 is the fraction of dielectric area involved (assumed to be 0.01)
A_D is the dielectric area (cm^2)

(2) The square wave approximation of the voltage transient is assumed to be the satellite ground potential at the time of discharge over the discharge period given above.

All of the voltage values and capacitance to space (C_s) are available from the NASCAP analysis. Dielectric capacitances can be computed from parallel plate formulas using values of dielectric constant and dimensions used in the NASCAP analysis.

This criteria can be applied to the SCATHA discharge transient considered in the previous section. The discharge was assumed to be triggered because the probe tip (metallic area) became more negative than the surrounding dielectric - exceeded breakdown initiation criteria a). In this case the probe tip was capacitively coupled to the spacecraft structure so that the transient response of the external structure could be determined for the selected value of coupling. The computation proceeds as follows:

(a) The capacitances are:
- Probe tip to space: 7.8×10^{-11} F
- Object to space: 1.2×10^{-10} F
- Probe tip to object: 2×10^{-10} F (value arbitrarily chosen)

(b) Charge lost:
$\Delta Q_1 = C_s \Delta V = 7.84 \times 10^{-11} \times 4720 = 0.37$ μC (charge lost from probe tip)
$\Delta Q_2 = K C_D \Delta V = 0.003 \times 4.2 \times 10^{-9} \times 200 =$ 0.0025 μC (charge lost from surrounding dielectric)
$\Delta Q_L = 0.37$ μC

(c) Pulse duration:
$\Delta t = 0.02\ (0.01 \times 170)^{1/2} = 26$ nsec
where area of dielectric boom was used.

(d) Current and voltage transients (see fig. 10):
$\Delta I = (0.37 \times 10^{-6})/(26 \times 10^{-9}) = 14.2$ A
$\Delta V_{probe} = 4720$ volts in 26×10^{-9} sec

(a) Structure response: If the response of the spacecraft to the discharge is simply by capacitive coupling, then

$$C_S \left(\frac{dV}{dt}\right)_{structure} = C_T \left(\frac{dV}{dt}\right)_{tip}$$

or

$$\Delta V_{structure} = \frac{C_T}{C_S} \Delta V_{tip} = \frac{7.8\times10^{-11}}{1.2\times10^{-10}} 4720$$

$$= 3000 \text{ volts}$$

This can be compared to the computer model predictions of the previous section. Since the structure potential was -3740 volts before discharge, the 3000 volt change would cause the structure to go to -740 volts. The code value was -725 volts. Hence, the NASCAP discharge switch routine incorporates the essence of the proposed process.

What has been presented here must be considered a preliminary attempt to formulate a usable guide for analyzing satellite designs. It is based on the idea that breakdowns occur early in the mission and does not consider any effects of dielectric aging or ground break-up that may occur with time in space. The process proposed here only approximates any effect of charges being redeposited on the dielectric. The use of a 1-percent loss with only 1/3 escaping may compensate for this effect, but it could introduce errors.

APPLICATION OF DISCHARGE MODEL

In this section the proposed discharge model is applied in a design study of a three-axis stabilized geosynchronous satellite. The NASCAP model of this satellite is shown in figure 11. It has two large, sun-tracking solar array wings and a central spacecraft body. The overall dimensions are 9 m across the wings by 2.4 m across the body. The model has 470 exposed surfaces and each square in the model is 0.3 by 0.3 m.

The solar array wings are each 3 by 1.8 m. They are modeled as thin, flat plates with 0.015 cm (6 mil) silica cover slides on the sun-facing side and 0.010 m (4 mil) Kapton substrates. This represents a flexible substrate solar array system capable of producing a total power output of about 1 kW. This array is assumed to be operating such that one wing is at +25 volts with respect to the spacecraft body while the other is at -25 volts when the array is sunlit. In eclipse conditions the array voltages are set to zero. The interconnects between the solar cells are modeled as silver patches (minimum resolution in NASCAP is one surface cell). These metallic patches represent about 10 percent of the total array area which is a reasonable approximation to the actual exposed metallic area.

The spacecraft body is modeled as an octagon 1.8 by 1.5 m deep. On the earth-facing side are two antennas modeled as octagons 0.9 by 0.3 m high. The sides of these antennas are covered by a grounded thermal blanket with 0.010 cm Kapton outer layer. The antenna cover is plain Kapton which can float electrically. On the opposite end of the body is an apogee insertion motor enclosure modeled as an octagon 1.2 by 0.6 m deep. The end is assumed covered by pure aluminum. The rest of the exposed surfaces of the spacecraft body are covered by 0.010 cm Kapton, 0.014 cm Silica (OSR simulation), or pure aluminum patches.

The struts holding the solar arrays to the body are modeled as a dielectric material with a low secondary yield. A probe has also been added to the body. This probe has an unspecified purpose and is modeled as having an aluminum tip with the quasi-dielectric body. Furthermore this probe is assumed to be very weakly capacitively coupled to the body.

A charging simulation was conducted using a moderate substorm from the design environment specification (Ref. 20). Twelve minutes of sunlight charging (with sunlight incident at 27° relative to the solar array normal) were simulated followed by an additional 12 minutes in eclipse. The charging history of selected surfaces is shown in figure 12.

This figure illustrates the differences between absolute, differential, and barrier-dominated charging (Ref. 8). In sunlight the charging of the structure ground starts only after differential charging of shaded insulators and proceeds at a slower rate than the insulators. Upon entering eclipse the potential of the system as a whole drops; the existing differential voltages are maintained (absolute charging). Then, differential charging resumes. The potential values reached in this charging event (both sunlit and eclipse conditions) are controlled by the voltage barriers built-up from the charging of the large, shaded Kapton substrates of the solar array. As these surfaces become more negative, electric fields expand, surrounding the satellite and controlling the incoming flux, the photo- and secondary emission (barrier-dominated charging).

A detailed review of the NASCAP graphics output indicates areas where discharges may occur. The predicted voltage profiles around the satellite are shown in figure 13 for sunlight charging after 12 minutes (720 sec). As shown in the front view the potentials tend to decay from the shaded Kapton (-5400 V). However, there are inflection points in the arrays and the center of each wing is at a positive potential with respect to ground (a condition which promotes discharges). The gradients from the array edges towards the center are also severe (as indicated by the number of lines grouped in a small area). These solar array differential voltages can be more severe if it is assumed that the cover slides have a high yield, magnesium fluoride, anti-reflecting coating instead of plain glass (Ref. 29). There are also inflection points between Kapton surfaces and both sunlit and shaded OSR's on the spacecraft body.

The side view of this figure indicates a possible problem at the solar array outer ends. Strong gradients exist and if there is an exposed metallic area, then breakdowns could occur there. On the spacecraft body there are strong gradients at the interface with the apogee motor. However, unless there is a seam or exposed metal edge in the region, the differential voltages are not sufficient to cause dielectric punch-through breakdowns. It should be pointed out that computer graphics tends to average equipotentials over the surface areas even when the surface is a grounded metallic area. This can lead to overlooking possible problems. The entire end of the motor case is supposed to be at ground potential. Hence, all voltage lines should terminate on the dielectric edge which pro-

duces a strong electric field at this point. This concentration is not apparent in the computer graphics and illustrates the need for care and diligence in interpreting computer outputs.

For eclipse charging conditions, the computed voltage profiles at about 800 seconds are shown in figure 14. The possible discharge areas are the solar array wing tips, all Kapton-metal interfaces, probe tip - dielectric boom interface and solar array cell - interconnect gaps. Breakdown characteristics can be estimated for both sunlight and eclipse charging conditions by following the procedure given in the discharge guideline. This procedure is applied to a possible discharge involving a single NASCAP cell area on the solar array (positive differential voltage breakdown criteria) and at a Kapton-metal interface (strong negative electric field criteria). These would be the transient characteristics at the discharge site and would serve as inputs to another code to compute system response.

Solar array gap breakdown: The satellite capacitance to space is computed to be 2.1×10^{-10} farads. The ground potentials are about -3 kV in sunlight charging conditions and about -9 kV in eclipse charging conditions. This results in charge losses of 0.63 and 1.9 μC, respectively. The capacitance of the block of solar cells in the 0.3 by 0.3 m NASCAP square is about 2×10^{-8} farad and the differential voltage (maximum) is about 500 volts in sunlight and about 1000 volts in eclipse. Under the criteria that 0.3 percent of the charge stored on the dielectric is also lost, then an additional 0.03 μC should be added for sunlight charging and 0.06 μC added for eclipse charging. The resulting total charge lost would be 0.66 μC for sun charging and 1.96 μC for eclipse charging. The square wave approximations for the voltage and current transients of this discharge source are shown in figure 14 (based on a computed pulse duration of 60 nsec for the assumed one surface cell breakdown) in both sunlight and eclipse conditions.

Kapton-metal interface breakdown: The charge contribution from the breakdown of the satellite to space capacitor is the same as above. The differential voltage on the shaded Kapton is about 2.5 kV for both sunlit and eclipse charging conditions. Since the Kapton capacitance per NASCAP square is about 2×10^{-8} farad, the total charge lost to space is 0.78 μC for sunlight charging and 2.0 μC for eclipse charging. The voltage and current transients for this discharge are similar to those shown in figure 15.

It is apparent that the probe tip would trigger a discharge as it entered eclipse and produce results similar to that of the SCATHA model study. Hence, upon entering eclipse one could antitipate an initial discharge due to the weakly coupled probe and have this followed by a differential voltage discharge caused by voltage gradients in the array or thermal blankets. The final assessment of any hazard to satellite systems requires using these transients as inputs to computational schemes to determine the structure and harness coupling possible. Modifications to the design, filtering or ignoring the charging possibilities could then be decided (Ref. 34).

CONCLUDING REMARKS

The question of environmentally-induced discharge hazards to spacecraft systems has long been debated. Initial studies indicated that the large area, charge clean-off, discharges observed in laboratory simulation could occur in space substorm encounters. The hazard from this type of "big-bang" discharge was obvious; many satellites should have been destroyed. This did not occur. Transients were detected on satellite surfaces and on internal electrical harnesses. The only recognizable hazards appeared to be anomalous electronic switching and noisy telemetry.

Data from spacecraft seemed to indicate that differential charging was controlled by voltage barriers and could not reach the levels required to obtain the big bangs. Analytical modeling techniques reached a state of maturity to predict reliably that known substorms could not produce sufficient differential voltages to trigger a major discharge. This focused attention on the "little bangs"; those irritating occurrences that had been previously ignored in laboratory studies. This has led to different concepts for discharge initiation and subsequent low energy pulses.

In this paper a discharge process is proposed. The trigger conditions postulated are: a negative exposed metallic surface surrounded by a less negative dielectric and a large voltage gradient at a dielectric/metal interface. Both of these conditions are essentially gap phenomenon and are based on laboratory data. Analysis of SCATHA data for a discharge occurrance seems to substantiate the postulation. Surface discharges cause a small transient charge transfer to space which results in voltage transients. A method of computing these transients has been developed based on the charge lost through the capacitance to space and a fraction of charge stored in the dielectric at the discharge source. This computation results in an estimate of the discharge transients at the discharge site and can be used as inputs for coupling code analysis of structure/system response. As an example, the transient computations have been applied to a three-axis stabilized, geosynchronous satellite for both sunlight and eclipse charging. The energy of the transient pulses were about 1 mjoule for sunlight discharge and 8 mjoule for eclipse. Changing of selected coatings on the satellite would relive the stress.

The proposed process and computational scheme given here is preliminary. It is based on available information and seems to explain some of the occurrances on satellite. As more data becomes available, the model will be improved.

REFERENCES

1. Rosen, A. (Ed.) 1976, Spacecraft Charging by Magnetospheric Plasmas, N.Y., AIAA, 3-14.

2. DeForest, S. E. 1972, Spacecraft Charging at Synchronous Orbits, J. Geophys. Res. 77 (4), 651-659.

3. DeForest, S. E. & McIlwain, C. E. 1971, Plasma Clouds in the Magnetosphere, J. Geophys. Res. 76 (16), 3587-3611.

4. Garrett, H. B. 1979, Modeling of the Geosynchronous Plasma Environment, Spacecraft Charging Technology - 1978, Colorado Springs 31 Oct.-2 Nov. 1978, NASA CP-2071/AFGL TR-79-0082, 11-22.

5. Mullen, E. G. et al. 1981, P78-2 SCATHA Environmental Data Atlas, Spacecraft Charging Technology - 1980, Colorado Springs 12-14 Nov. 1980, NASA CP-2182/AFGL TR-81-0270, 802-813.

6. Nanevicz, J. E. & Adamo, R. C. 1977, Transient Response Measurements on a Satellite System, Proceedings of the Spacecraft Charging Technology Conference, Colorado Springs 27-29 Oct. 1976, AFGL TR-77-0051/NASA TM X-73537, 723-734.

7. Stevens, N. J. et al. 1977, Summary of CTS Transient Event Counter Data After One Year of Operation, IEEE Trans. Nucl. Sci. NS-24 (6), 2270-2275.

8. AIAA 82-0273 1982, Evolution of Spacecraft Charging Technology, by Purvis, C.

9. Grasd, R. (Ed.) 1973, Photon and Particle Interactions with Surfaces in Space, Dordrecht, D. Reidel Pub. Co., 277-308.

10. Rosen, A. (Ed.) 1976, Spacecraft Charging by Magnetospheric Plasmas, N.Y., AIAA, 253-275.

11. Rosen, A. (Ed.) 1976, Spacecraft Charging by Magnetospheric Plasmas, N.Y., AIAA, 15-30.

12. Stevens, N. J. 1981, Analytical Modeling of Satellites in Geosynchronous Environment, Spacecraft Charging Technology - 1980, Colorado Springs 12-14 Nov. 1980, NASA CP-2182/AFGL TR-81-0270, 717-729.

13. Mizera, P. F. & Boyd, G. M. 1981, Satellite Surface Potential Survey, Spacecraft Charging Technology - 1980, Colorado Springs 12-14 Nov. 1980, NASA CP-2182/AFGL TR-81-0270, 461-469.

14. Olsen, R. C. et al. 1981, Observation of Differential Charging Effects on ATS-6, J. Geophys. Res. 86 (A8), 6809-6819.

15. Katz, I. et al. 1979, The Capabilities of the NASA Charging Analyzer Program, Spacecraft Charging Technology - 1978, Colorado Springs 31 Oct.-2 Nov. 1978, NASA CP-2071/AFGL TR-79-0082, 101-122.

16. SSS-R-78-3739 (Systems Science and Software) 1978, NASCAP User's Manual - 1978, by Cassidy, J.

17. SSS-R-79-3904 (Systems Science and Software) 1979, Extension, Validation, and Application of the NASCAP Code, by Katz, I. et al.

18. SSS-R-4847 (Systems Science and Software) 1981, Additional Application of the NASCAP Code - Vol. I: NASCAP Extension, by Katz, I. et al.

19. AIAA Paper 80-0040 1980, Configuration Effects on Satellite Charging Response, by Purvis, C.

20. Stevens, N. J. 1981, Use of Charging Control Guidelines for Geosynchronous Satellite Design Studies, Spacecraft Charging Technology - 1980, Colorado Springs 12-14 Nov. 1980, NASA CP-2182/AFGL TR-81-0270, 789-801.

21. Stevens, N. J. et al. 1977, Testing of Typical Spacecraft Materials in a Simulated Substorm Environment, Proceedings of the Spacecraft Charging Technology Conference, Colorado 27-29 Oct. 1976, AFGL TR-77-0051/NASA TM X-73537, 431-458.

22. Osgood, R. N. 1981, Operational Status of the Space Test Program P78-2 Spacecraft and Payloads, Spacecraft Charging Technology - 1980, Colorado Springs 12-14 Nov. 1980, NASA CP-2182/AFGL TR-81-0270, 365-369.

23. Vampola, A. L. 1981, P78-2 Engineering Overview, Spacecraft Charging Technology - 1980, Colorado Springs 12-14 Nov. 1980, NASA CP-2182/AFGL TR-81-0270, 439-460.

24. AIAA Paper 80 0334 1980, Natural and Artificial Charging: Results from the Satellite Surface Potential Monitor Flown on P78-2, by Mizero, P. F.

25. Koons, H. C. 1981, Aspect Dependence and Frequency Spectrum of Electrical Discharges on the P78-2 (SCATHA) Satellite, Spacecraft Charging Technology - 1980, Colorado Springs 12-14 Nov. 1980, NASA CP-2182/AFGL TR-81-0270, 478-492.

26. Purvis, C. K. & Staskus, J. V. 1981, SCATHA SSPM Response: NASCAP Predictions Compared with Data, Spacecraft Charging Technology - 1980, Colorado Springs 12-14 Nov. 1980, NASA CP-2182/AFGL TR-81, 0270, 592-607.

27. AIAA Paper 82-0269 1982, Validation of the NASCAP Model Using Satellite Data, by Stannard, P. R. & Katz, I.

28. Inouye, G. T. & Sellen, J. M. 1979, TDRSS Solar Array Arc Discharge Tests, Spacecraft Charging Technology - 1978, Colorado Springs 31 Oct.-2 Nov. 1978, NASA CP-2071/AFGL TR-79-0082, 834-852.

29. Staskus, J. V. & Roche, J. C. 1981, Testing of a Spacecraft Model in a Combined Environment Simulator, IEEE Annual Conference on Nuclear and Space Radiation Effects, Seattle WA 21-24 July 1981.

30. Stevens, N. J. et al. 1978, Insulator Edge Voltage Gradient Effects in Spacecraft Charging Phenomena, IEEE Trans. Nucl. Sci. NS-25 (6), 1304-1312.

31. Frederickson, A. R. 1981, Bulk Charging and Breakdown in Electron Irradiated Polymers, Spacecraft Charging Technology - 1980, Colorado Springs 12-14 Nov. 1980, NASA CP-2182/AFGL TR-81-0270, 33-51.

32. Flanagan, T. M. et al, 1979, Effect of Laboratory Simulation Parameters on Spacecraft Dielectric Discharges, IEEE Trans. Nucl. Sci. NS-26 (6), 5134-5140.

33. Aron, P. R. & Staskus, J. V. 1979, Area Scaling Investigations of Charging Phenomena, Spacecraft Charging Technology - 1978, Colorado Springs 31 Oct.-2 Nov. 1978, NASA CP-2071/AFGL TR-79-0082, 485-506.

34. NASA TM-82781 1982, Design Practices for Controlling Spacecraft Charging Interactions, by Stevens, N. J.

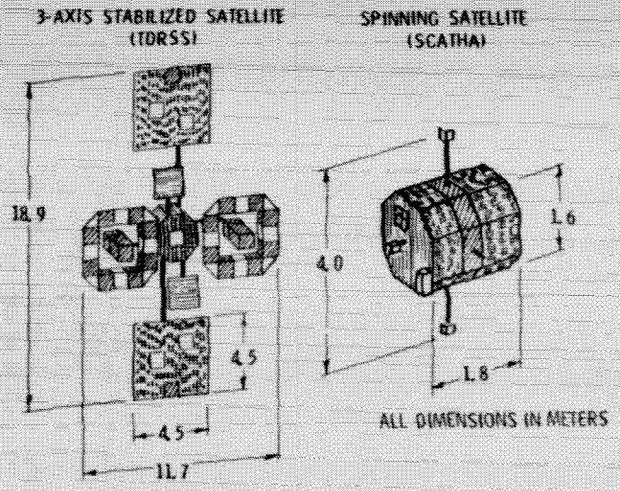

Figure 1. - NASCAP models of geosynchronous satellites.

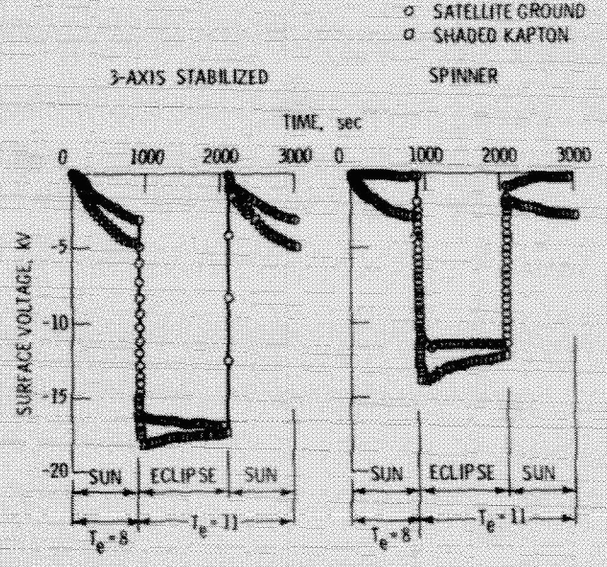

Figure 2. - Predicted behavior in design substorm effect of stabilization.

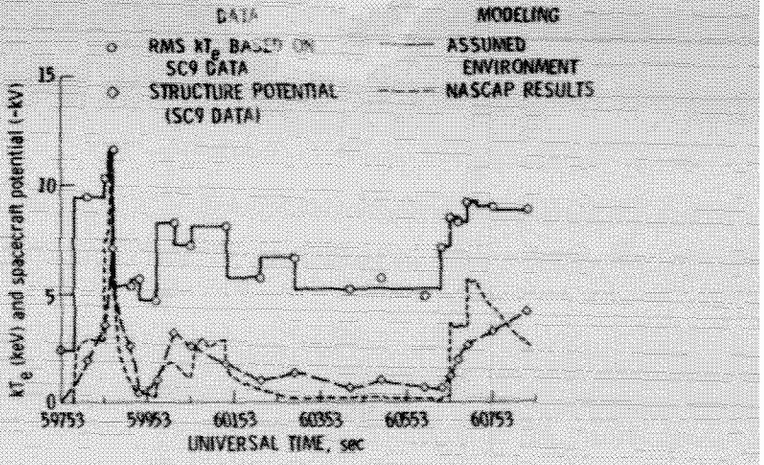

Figure 3. - SCATHA day 87 1979.

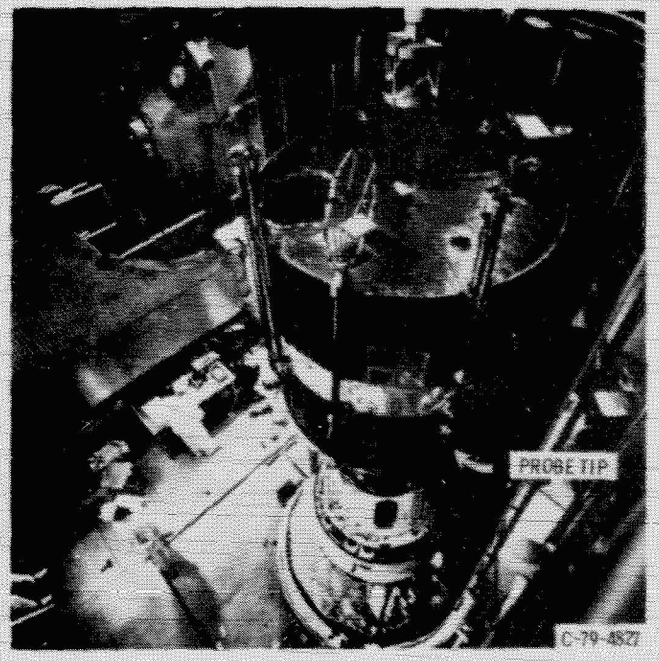

Figure 4. - Scatha Satellite. (Prelaunch Checkout).

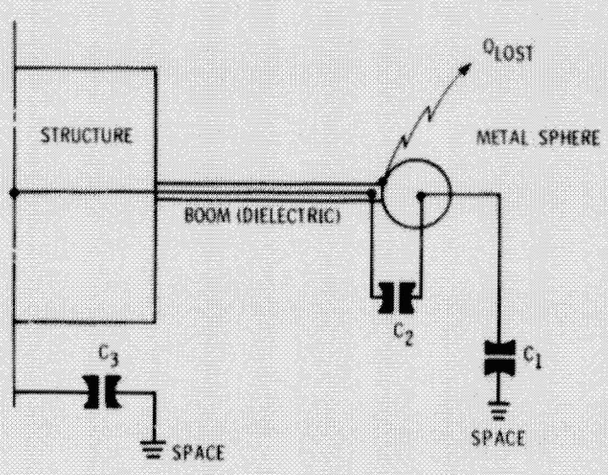

Figure 5. - Proposed capacitor model for discharge SCATHA satellite.

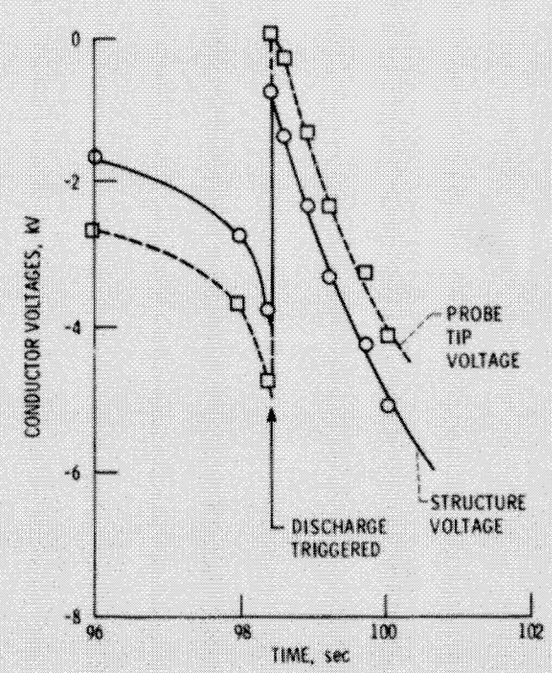

Figure 6. - Simulated discharge transient (NASCAP). Charge lost to space from probe tip, 0.37 μC.

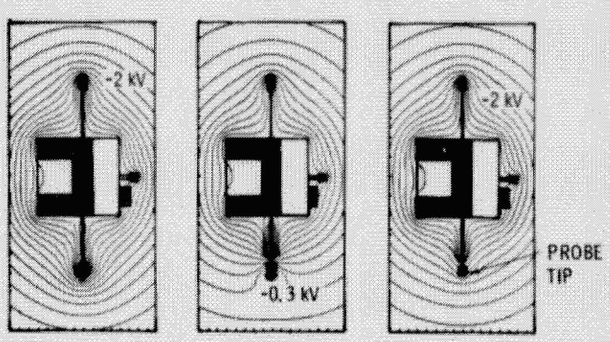

(a) Equipotential lines at 200-V steps. Time, 98.4 sec (prior to discharge); structure, -3.74 kV; probe tip, -4.72 kV.

(b) Equipotential lines at 50-V steps. Time, 98.4 sec (discharge); structure, -0.73 kV; probe tip, +15 V.

(c) Equipotential lines at 200-V steps. Time, 99.2 sec (recovery); structure, -3.29 kV; probe tip, -2.3 kV.

Figure 7. Predicted voltage profiles during discharge simulation. Charge lost to space, 0.37 μC.

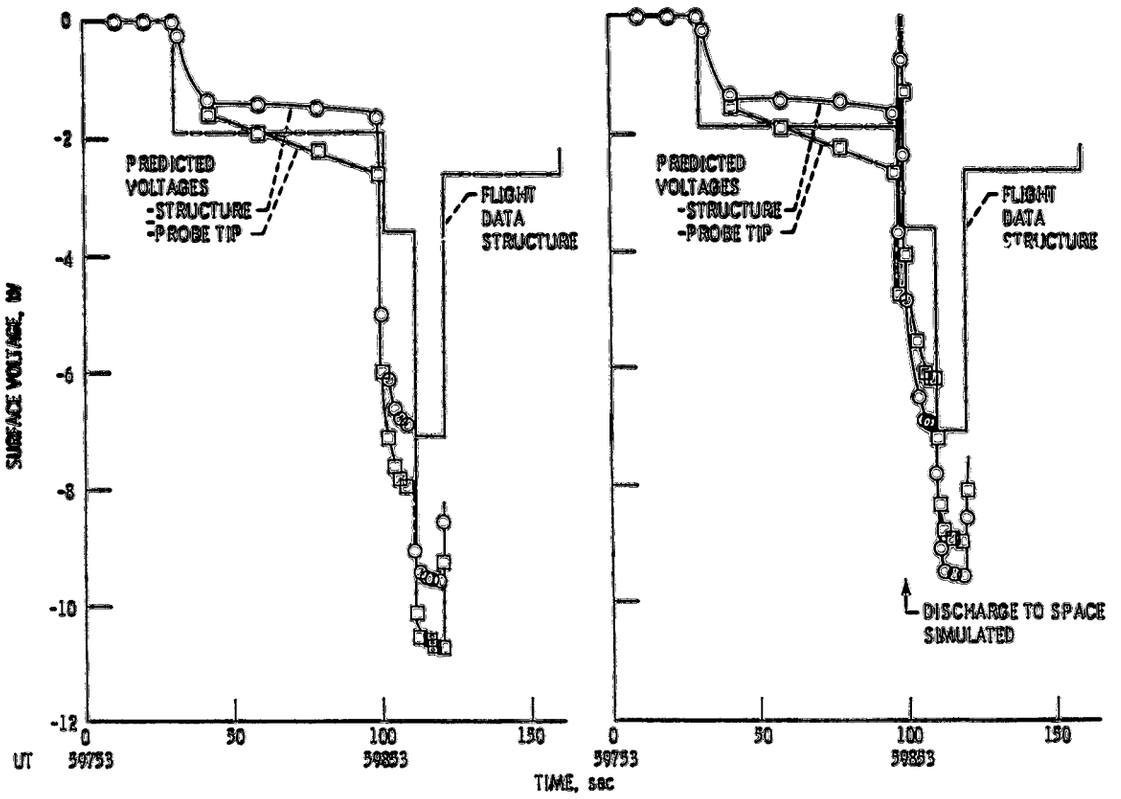

(a) Without discharge simulation.

(b) With discharge simulation.

Figure 8. - Predicted charging history for eclipse substorm encounter (SCATHA model - March 28, 1979).

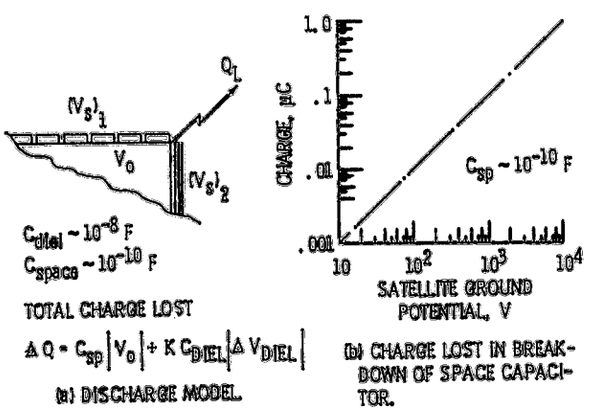

(a) DISCHARGE MODEL.

(b) CHARGE LOST IN BREAKDOWN OF SPACE CAPACITOR.

Figure 9. - Surface discharges.

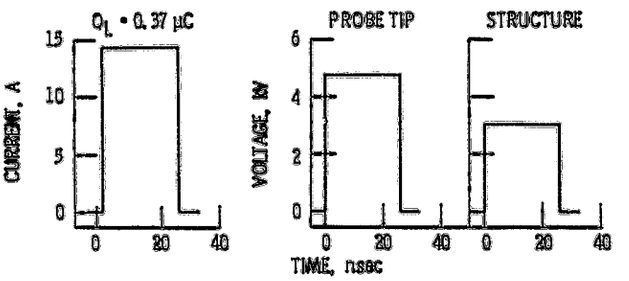

Figure 10. - Predicted transients - SCATHA discharge at discharge site (proposed criteria).

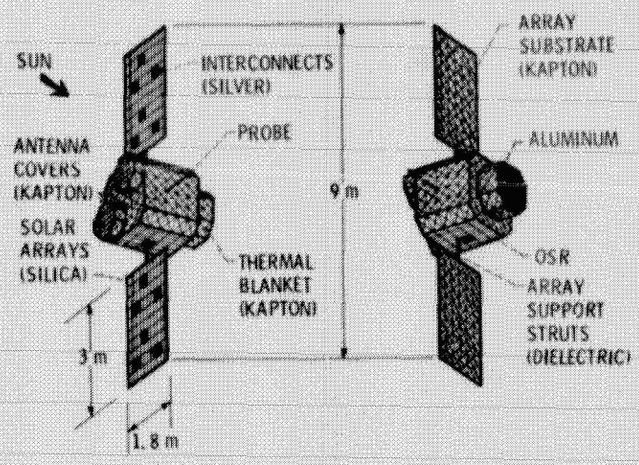

Figure 11. - Three-axis stabilized geosynchronous satellite (design guideline study).

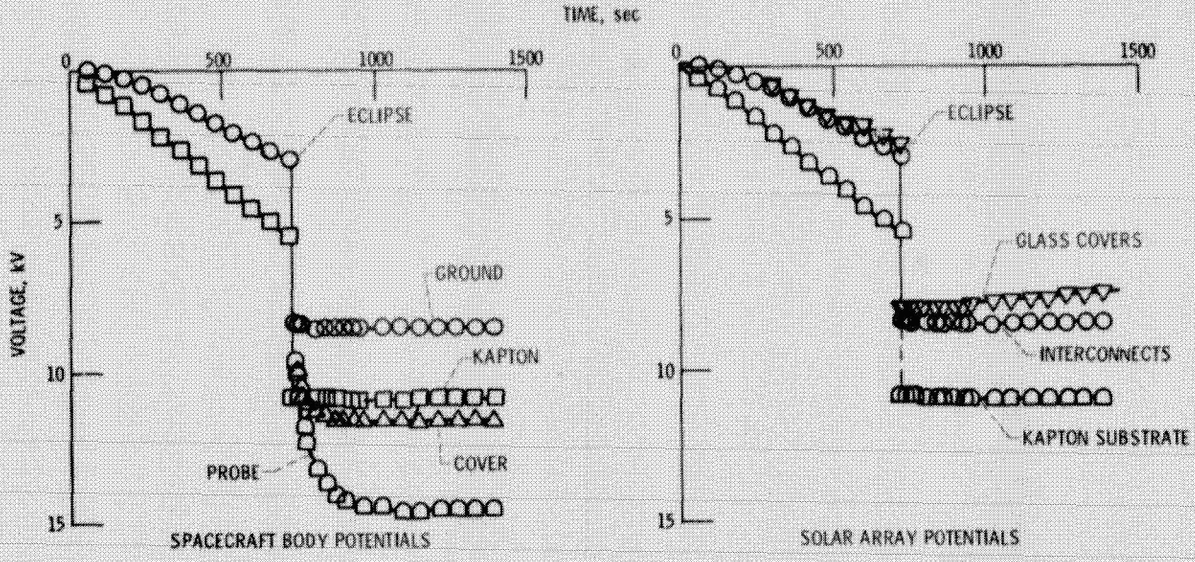

Figure 12. - Preliminary satellite design study - surface charging history; phase 1 substorm.

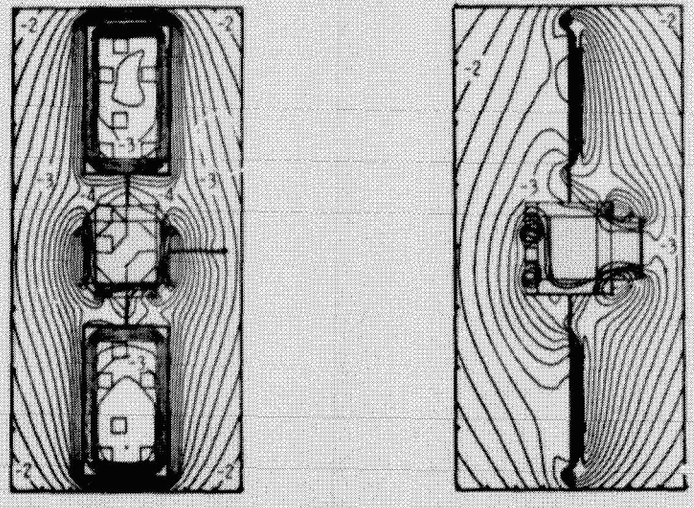

Figure 13. - Voltage profiles - sun charging; equipotentials at 0.2 kV; spacecraft ground -2.99 kV.

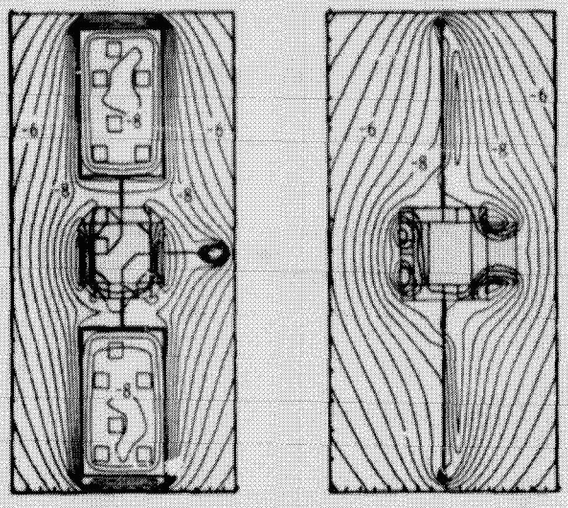

Figure 14. - Voltage profiles - eclipse charging - satellite precharged. Equipotentials at 0.5 kV; spacecraft ground, -8.48 kV.

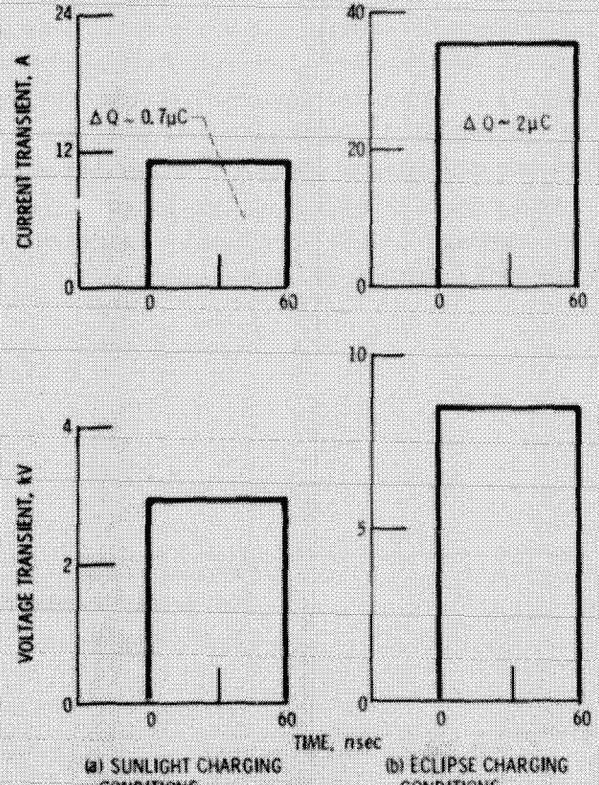

(a) SUNLIGHT CHARGING CONDITIONS.

(b) ECLIPSE CHARGING CONDITIONS.

Figure 15. - Anticipated discharge pulses.